Shahrood University of Technology
Iranian Society of Mining Engineering (IRSME)
Journal of Mining and Environment (JME)
journal homepage: www.jme.shahroodut.ac.ir
THOMSON REUTERS
Vol. 10, No. 3, 2019, 667-678.
DOI: 10.22044/jme.2019.7915.1658

Ant colony algorithm as a high-performance method in resource estimation using LVA field; A case study: Choghart Iron ore deposit

H. Moeini and F. Mohammad Torab*

Department of Mining and Metallurgical Engineering, Yazd University, Yazd, Iran

Received 29 December 2018; received in revised form 5 April 2019; accepted 12 April 2019

Keywords

Ant Colony Algorithm

Locally Varying Anisotropy

Resource Estimation

Kriging

Choghart Deposit

Abstract

Kriging is an advanced geostatistical procedure that generates an estimated surface or 3D model from a scattered set of points. This method can be used for estimating resources using a grid of sampled boreholes. However, conventional ordinary kriging (OK) is unable to take locally varying anisotropy (LVA) into account. A numerical approach has been presented that generates an LVA field by calculating the anisotropy parameters (direction and magnitude) in each cell of the estimation grid. After converting the shortest anisotropic distances to Euclidean distances in the grid, they can be used in variography and kriging equations (LVAOK). The ant colony optimization (ACO) algorithm is a nature-inspired metaheuristic method that is applied to extract image features. A program has been developed based on the application of ACO algorithm, in which the ants choose their paths based on the LVA parameters and act as a moving average window on a primary interpolated grid. If the initial parameters of the ACO algorithm are properly set, the ants would be able to simulate the mineralization paths along continuities. In this research work, Choghart iron ore deposit with 2,447 composite borehole samples was studied with LVA-kriging and ACO algorithm. The outputs were cross-validated with the 111,131 blast hole samples and the Jenson-Shannon (JS) criterion. The obtained results show that the ACO algorithm outperforms both LVAOK and OK (with a correlation coefficient value of 0.65 and a JS value of 0.025). Setting the parameters by trial-and-error is the main problem of the ACO algorithm.

1. Introduction

Kriging-based linear estimators can efficiently evaluate unknown values in a region using some data from neighboring areas. Although they perform better than many other estimation algorithms, in case of locally varying anisotropy, they cannot model the resource properly. Anisotropy is a phenomenon that occurs in many mineral deposits such as bedded, layered, folded or vein-type structures. Conventional estimation methods assume a constant anisotropy value representing a global unidirectional continuity within Euclidean distances. This assumption is not valid where there is a locally varying anisotropy (LVA) due to non-linear features that violate the assumptions of conventional kriging equations.

Researchers have proposed different solutions to model LVA in resource estimation. Some used kriging with a local search that applied anisotropy direction at the estimation points to its local neighborhood [1-3]. In another variant, the local anisotropy has been calculated from the available data and incorporated to accurately reproduce curvilinear structures using an iterative image analysis technique [4]. Some researchers have tried to model LVA directions in 1D spectral simulations on features [5] or applied multi-dimensional scaling (MDS) [6-12] as well as considering a spatial kernel method or weighted moving window average on features whose parameters have been varied locally

* Corresponding author: fmtorab@yazd.ac.ir (F. Mohammad Torab).

[13-16]. They were limited to smaller models and were not practical for larger grids. Kernels also require a locally stationarity assumption during estimations. In order to model curvilinear directions, 'stream distances' have been used [16-22] to ignore indefinite systems of kriging equations that result from considering an invalid distance metric in covariance functions.

In a recent publication, a numerical approach has incorporated LVA directions in ordinary kriging equations [23]. Taking the sample points as the nodes of a graph, the authors have calculated the shortest anisotropic distances using the LVA parameters, and after converting to isotropic coordinates and applying MDS, they have rescaled the distances to Euclidean. In fact, they simplified the curvilinear continuity paths into the segmented linear ones. These distances could then be used in a conventional kriging procedure.

ACO is a nature-inspired metaheuristic algorithm that models the foraging of ants for optimizing a system [24]. It was first used in different optimization problems [25-30], and then extended to image analysis where ants could react and adapt to any type of digital habitat [31].

Various researchers have applied neural networks to ore deposit grade estimation [32-34]. They have developed different architectures and arrangements of neurons to detect the data patterns. However, neural networks have numerous settings and conditions to be set. Arranging the neurons and their connections is also laborious. Furthermore, a trained network would not be applicable to any other case. Recently, the ACO algorithm has successfully detected univariate geochemical anomalies based on a 2D grid element map [35].

This paper presents the application of ACO to estimate mineral resources with a locally varying anisotropy. In this research work, we used the Chen & An [35] method of anomaly detection using ACO and modified it in a way to be able to change the values in 2D cells of a geochemical map or 3D blocks of a resource model concerning LVA parameters. New modules were designed and added to the code to make the ants act as modifying agents on voxels. We believe that this is the first time this approach has been taken.

In order to evaluate the performance of the newly developed method, we applied it to 3D data of borehole samples at Choghart iron deposit and verified the results with blast hole samples. The same procedure was carried out with LVA- and conventional kriging. Comparing the results obtained for LVA-, conventional kriging, and ACO estimation with blast hole samples showed that the latter outperformed the others. The Jenson-Shannon (JS) divergence criterion was also applied to these methods to evaluate the similarity of the distribution of the estimated data versus the raw data. This criterion has been used by others to compare the results of applying a newly developed filter to that of the conventional algorithm in multiple-point statistics [36].

A drawback of LVA-kriging is its variography that, like conventional kriging, depends on the user's experience, sufficient samples, and many other practical factors. ACO does not require variography or data preparation, though it requires some initial parameters to initiate trial-and-error. The computer code was scripted in the MATLAB software.

2. Choghart iron ore deposit

The Choghart iron ore deposit is located 12 km NE Bafq and 125 km SE Yazd. Choghart current mining depth is about 900 m above the sea level. Today, it is excavated by an open-pit on benches of 12.5 m height.

The form of the main orebody at Choghart is a roughly vertical, discordant, pipe-shaped body. The orebody has been explored to a depth of 600 m, where it appears to intertwine with metasomatized and brecciated volcanic and dolomitic wall-rock units of the Early Cambrian Esfordi Formation. The geological map and cross-section of the deposit (Figure 1) reveal that the Esfordi Formation unconformably overlies the high-grade metamorphic Precambrian basement of the Boneh-Shurow Complex, and a highly metasomatized magmatic rock with altered dolomite fragments of the Esfordi Formation is the main host to the orebody. The igneous rock in the core of the deposit is strongly albitized. All rocks of the complex display extensive mineralogical, textural, and compositional diversity, with varying degrees of hydrothermal alterations. Several mafic dikes cut the orebody and country rocks in different directions, and make grade discontinuities throughout the deposit [37, 38].

The massive magnetite forms the lower part of the Choghart orebody with accessory minerals including apatite, pyrite, amphiboles, calcite, talc, quartz, monazite, and allanite. The oxidation zone extends to a 150 m depth from growing martitization in depth to complete replacement of magnetite by martite near the surface.

Hematite is the secondary mineral, though some primary hematite has been found in the drill cores.

Some goethite and hydrous iron oxides also occur near the surface without any evidence in depth. Apatite is the most abundant gangue mineral at Choghart. It occurs in varying proportions with magnetite. According to the composition and degrees of oxidation, the iron ore of Choghart is of low-sulfur type with about 90% of non-oxidized magnetite ore and more than 65% of low-phosphorus type. The estimated reserve for Choghart has been reported to be 215.7 Mt on the basis of a 20%-cut-off-grade for the total iron [39].

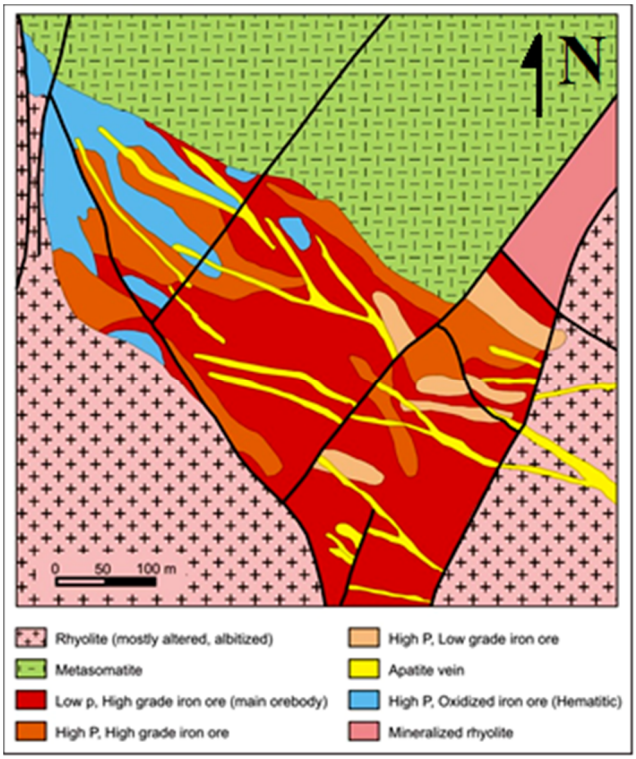

Figure 1. Simplified geological map of the Choghart deposit [37, 39].

3. Methods

3.1. Kriging with locally varying anisotropy (LVA)

Anisotropy is modeled using an ellipsoid to represent the directional continuity of a geo-variable. In conventional kriging, anisotropy is assumed constant through the studied area. If local changes in the anisotropy direction and magnitude are observed in the studied area, they could improve the estimation process and produce more geologically realistic results [23].

The first step in LVA-kriging is to infer the LVA field of the studied area. An exhaustive LVA field in 2D is defined by the *major direction* (strike) and r_1 ratio (minor/major) for each cell of a gridded map of concentrations. In 3D, *semi-major* (dip) and *minor* (plunge) directions of continuity and r_2 ratio (semi/major) are added. The initial map or block model can be produced by simply interpolating the data using omnidirectional block kriging to give an overall view of the continuities. The map/volume is then blurred to be used in the automatic extraction of local anisotropy parameters. The blurring is a denoising or smoothing filter that highlights the continuous features of an image.

There are two methods of automatic LVA field extraction: 1) moment of inertia and 2) gradient principal component analysis (PCA). Both use a moving adaptive window over the initial map/blocks. The anisotropy parameters of each window in both methods are detected by eigenvalue decomposition of two tensors. The first is the moment of inertia of the covariance map of the window [40] and the second is PCA of the greyed image gradient over that window. The non-automatic method uses point sources; if the anisotropy parameters are sampled *in situ*, the LVA field can be interpolated throughout the sampling area (for further a reading on the methodology of LVA field extraction, see [41]).

The generated LVA field is then incorporated into kriging equations by calculating the non-linear shortest paths between points in the LVA field. The shortest path is measured by the anisotropic not the Euclidean distance between two points. The anisotropic distance between points 1 and 2 is calculated using the following equation [42]:

$$d_{12}=\sqrt{\left(\frac{d_x}{a_x}\right)^2+\left(\frac{d_y}{a_y}\right)^2+\left(\frac{d_z}{a_z}\right)^2}$$

where d_x is the distance and a_x is the range of anisotropy in the x direction. The larger the range in a particular direction is, the shorter the distance between points in that direction will be. In case of no anisotropy, the shortest distance is the direct path. However, because of anisotropy in most natural phenomena, the shortest distance makes a curvilinear path. One way to calculate these non-linear distances is to simplify the gridded data into a graph, where the nodes are the centers and the edges are the anisotropic distances of the grid cells/blocks. The distances between locations are calculated as the sum over all intersected blocks of a piecewise linear path between the nodes. When this optimum path is found, the resulting distance is used in the kriging and simulation processes [42].

Once embedded in a Euclidean space by L-ISOMAP scaling, an isotropic variogram (mostly exponential) can be modeled. The estimation process is like a conventional ordinary kriging algorithm that operates in the high-dimensional space as follows (for further reading see [23]):

- At every grid cell, the nearest N neighbors are determined.
- Then the required N by N distance matrix in the rescaled space is calculated.
- The covariance matrix is calculated using the modeled variogram and the distance matrix.
- The resulting conventional kriging system of equations is solved to determine the weights.
- The kriging mean and variance are calculated.

3.2. Ant colony system and block evaluation

The ACO algorithm, proposed by Dorigo [24], is based upon the swarm intelligence inspired by the nature. The principle behind such systems is the interaction between swarms of mobile agents using a simple communicator to find the optimum paths in foraging. The ants initially wander randomly when foraging, and when finding food source, return to their colony and lay down pheromone trails. Other ants that find the path will follow the trail, and when returning, reinforce it if they eventually find food. The pheromone trail will also start to evaporate over time. Therefore, the pheromone concentration varies from the initial random foraging route. The ants follow the routes with higher pheromone concentrations, and the pheromone is enhanced by the increasing number of ants. As time passes, more and more ants follow the same route, and it becomes the favored path. Thus some favorite routes are highlighted as the shortest or more efficient routes [43].

Two important factors involved in decoding this natural behavior to computer code are the 1) probability of choosing a route and 2) evaporation rate of pheromone. The probability of ants at a particular node *i* to choose the route from *i* to *j* is:

$$p_{ij}=\frac{\phi_{ij}^{\alpha}d_{ij}^{\beta}}{\sum_{i,j=1}^{n}\phi_{ij}^{\alpha}d_{ij}^{\beta}}.\quad \forall j\in A; j\notin TL_k$$

where $\alpha\geq 0$ and $\beta\geq 0$ are the influence parameters, ϕ_{ij} is the pheromone concentration in the route between node *i* and node *j*, and d_{ij} is the desirability of the same route [43]; *A* is a set of neighboring nodes and TL_k is the taboo list. The desirability can be defined using any heuristic formula. In this research work, d_{ij} is called '*LVA effect*' and set as:

$$\alpha=1;\beta=2;$$

$$d_{ij}=\left(2-\frac{\sum\left|lva(\theta)_i-lva(\theta)_j\right|}{S}\right)*\left(2-lva(r)_j\right)$$

where $lva(\theta)_i$ is the anisotropy angle parameters (i.e. strike, dip, plunge) of the LVA field in cell *i* and $lva(r)_j$ is the anisotropy ratio r_1 of the cell *j; S* is a normalization factor that is 540 for 3d and 360 for the 2d cases. This setting has the effect of directing the route selection along the anisotropic distance. The more two neighboring cells are aligned, the higher priority will the ants have to take that path.

At each iteration, the pheromone evaporates. When all the ants have completed their routes, pheromone trails on the path from node *i* to node *j* at iteration *t* are updated as [24].

$$\phi_{ij}(t+1)=\rho\phi_{ij}(t)+\Delta\phi_{ij}(t)$$

where ρ is the evaporation coefficient within the interval [0,1] and $\Delta\phi_{ij}(t)$ is the pheromone trail updated by all the *m* ants;

$$\Delta\phi_{ij}(t)=\sum_{k}^{m}\Delta\phi_{ij}^{k}(t)$$

$\Delta\phi_{ij}^{k}(t)$ is the pheromone trail updated by ant k if it moves from node i to node j, and it is defined as:

$$\Delta\phi_{ij}^{k}(t)=\frac{1}{L_k}$$

where L_k is the path length experienced by ant k. The shorter the path is, the more the pheromone trail is enhanced [35].

Ramos and Almeida [31] and Zhuang [46] used the ACO algorithm to extract image features. This idea was developed and applied successfully to detect anomalies in geochemical exploration [35]. The nodes are the cells or blocks of a gridded map or volume. In fact, the base map or block model is the one that is used in the LVA field inference, and here is updated by the ants.

In other words, all the ants of the colony move simultaneously toward adjacent grid points to find the anisotropic paths until the termination condition is satisfied. m ants are initially put into the non-empty grid points in random, and the pheromone trail on the path between grid points is set as a small positive constant value. After each iteration, the pheromone trail intensity on the path from each grid point to its neighbor is updated in order to record the accumulated experience of the ant colony during the iterative search process. The modified quantity of the pheromone trail intensity is determined by 1) the difference between the element concentration values of two adjacent grid points and 2) the number of ants that have experienced the path between two grid points in the current iteration [35].

In order to avoid visiting a grid point repeatedly during the search process, each ant has to memorize the visited grid points in a Taboo List. The length of the Taboo List is determined upon the behavior of the grid value; it should be defined short if the spatial distribution of the value is erratic. In this case, even small geochemical changes are expected to be properly tracked in the search procedure [35].

After the algorithm gets converged, all the ants of the colony become stationary during iteration and tend to gather in geochemically higher values in the grid map/block. If no more grid points are visited by the ants in the search process before the end of predefined iterations, the program terminates.

In a grid map, a weak fluctuation of interpolated concentration values in the vicinity of a grid cell may indicate a random variation that should be ignored in the path selection of an ant. Therefore, a fluctuation limitation, as a threshold, is defined for filtering random variations between any two adjacent grid points. If the maximum difference of concentration values between a current grid point and its neighbors is less than the threshold, the ant at a current grid point will randomly choose a neighboring grid point to move to [35].

During each iteration, the ants act as moving average windows on the visited cells/blocks and modify their values. The final values of the cells/blocks will be more continuous along the local anisotropies. The overall procedure can be repeated and eventually averaged in order to neutralize the impact of randomness on the outputs.

4. Cross-validation of results

4.1. Validating with blast holes

The most reliable validation of estimated values is to check them with their real ones. This could be done after sampling and analyzing the excavating benches, while drilling blast holes in them. The blast hole sample points that are located in an estimated cell/block are averaged and compared with its estimated value.

4.2. Jenson-Shannon (JM) divergence criterion

Another validation is to evaluate the similarity between the probability distributions using the relative entropy or Kullback-Leibler (KL) divergence. For probability distributions P and Q defined on the same probability space, the KL divergence from Q to P in continuous form is defined to be [44]:

$$D_{KL}(P\|Q)=\int_{-\infty}^{+\infty}p(x)\log\left(\frac{p(x)}{q(x)}\right)dx$$

where p and q denote the probability densities of P and Q of random variable x. In other words, it is the expectation of the logarithmic difference between the probabilities P and Q. A KL divergence of 0 indicates that the two distributions P and Q are identical. The JS divergence is a smooth symmetric version of KL, and is defined as [44]:

$$D_{JS}=\frac{1}{2}D_{KL}(P\|M)+\frac{1}{2}D_{KL}(Q\|M);\quad M=\frac{1}{2}(P+Q)$$

Due to the asymmetric behavior of KL, JS divergence was used instead as a criterion to compare the histograms of the estimated and true values [45].

5. Results

The data consisted of 2,413 composite borehole samples (Figure 2) that were analyzed for the Fe content (%). They were normalized with normal score transformation (NST) using the quantile-quantile approach to reduce the influence of negative skewness (Table 1). The transformed data was used in both LVA- and conventional kriging.

At first, the iron grade was estimated using ordinary kriging. The 3D anisotropic variography (Figure 3) and its parameters (Table 2) were used in the kriging process.

The resource volume was gridded into 25,760 blocks with *23*20*56* blocks of *25m*25m*10m* sizes in the x, y, and z directions according to specifications of the excavating benches. The grid was used in all estimations throughout this work. From all blocks, 7504 were within the convex hull of the borehole data, and were estimated by the three methods (Figure 4).

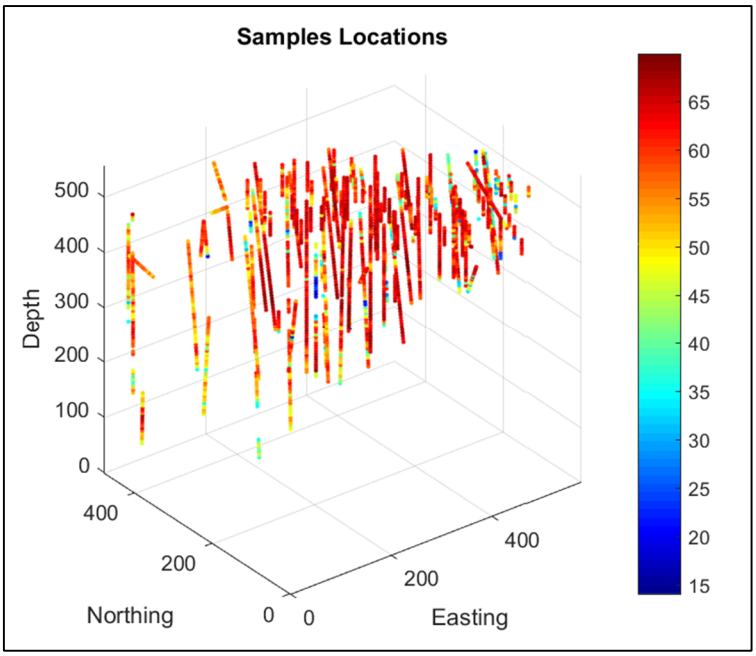

Figure 2. The location of borehole samples and their Fe (%) grade ranges.

Table 1. Descriptive statistics of borehole samples in raw and NST.

Fe	Min	Median	Mean	Max	SD	Skewness	Kurtosis	CV (%)
Raw data	14.105	60.828	57.796	69.88	9.136	-1.598	5.722	15.808
NST data	-3.534	0	0	3.534	1	0	2.987	Inf

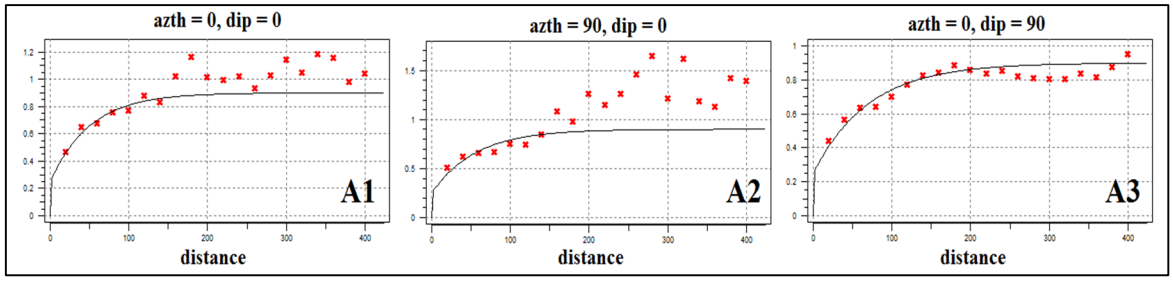

Figure 3. Variogram of borehole samples in 3 directions.

Table 2. Variogram parameters.

Variogram	Model: Exponential	Nugget effect: 0.25	Sill (Contribution): 0.65
Ranges	Max: 212 m	Medium: 168 m	Min 152 m
Angles	X:0	Y:90	Z:0

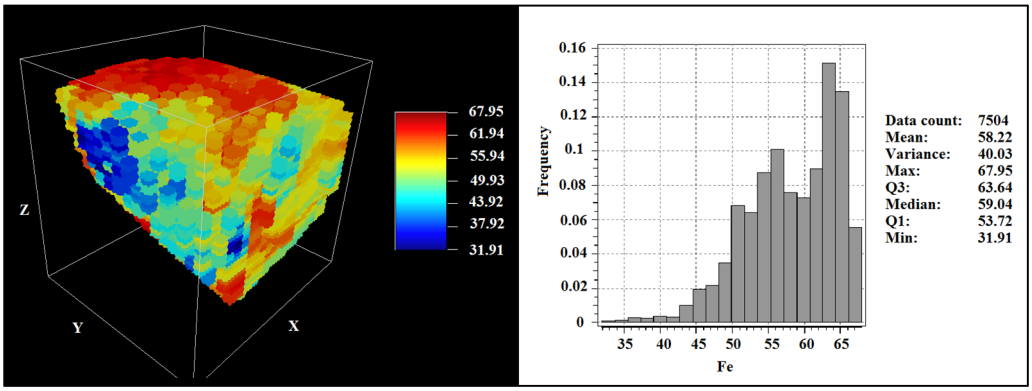

Figure 4. Left: Blocks of studied area estimated with ordinary kriging. Right: histogram of the estimated data.

The next step was estimating using LVA-kriging. To do this, an LVA field of the studied area was required. This was generated automatically by the moment of inertia method (Figure 5). Then the variography of the borehole samples was calculated using the LVA field parameters in each block, and an exponential model was fitted (Figure 6). Because of the L-ISOMAP scaling, the shortest path distances are converted to Euclidean, which makes the new estimation space isotropic. Therefore, the variography is done omni-directionally.

The modeled variogram parameters (Figure 6) were used in LVA-kriging and the blocks were estimated along the continuities of the deposit (Figure 7).

Finally, the ACO method was used by modifying the primary block model along the continuities using the LVA field parameters. The virtual ants were randomly put into the blocks and acted like moving average agents in their foraging routes. They selected the next block in their path based on the highest accordance between the LVA parameters of the next and current blocks. In each run, the overall procedure was repeated twice and the values were eventually averaged to reduce the randomness effect. The initial parameters of the ant colony algorithm were selected with trial-and-error. The obtained results were tested after each run with the JS and KL divergence criteria. The final set of initial parameters that gave the least JS value and best result (Figure 8) was 200 ants, 20000 iterations, 0.01 for pheromone trail, 0.05 for pheromone evaporation coefficient, 30 blocks for taboo path length, and 0.001 for fluctuation limitation.

Then the three methods were validated with 111,131 blast hole samples up to 200 m depth (20 bench levels) (Figure 9). The higher correlation means the better estimation and the more realistic values (Figure 10). Therefore, the ACO estimation performed better than the other methods.

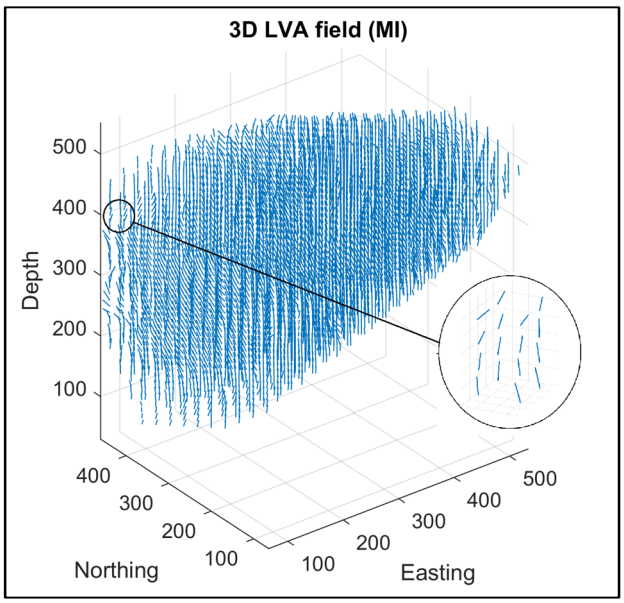

Figure 5. LVA field of the studied area. Anisotropy direction of each block is shown as direction of a line. The anisotropy ratios are proportional to the length of the lines.

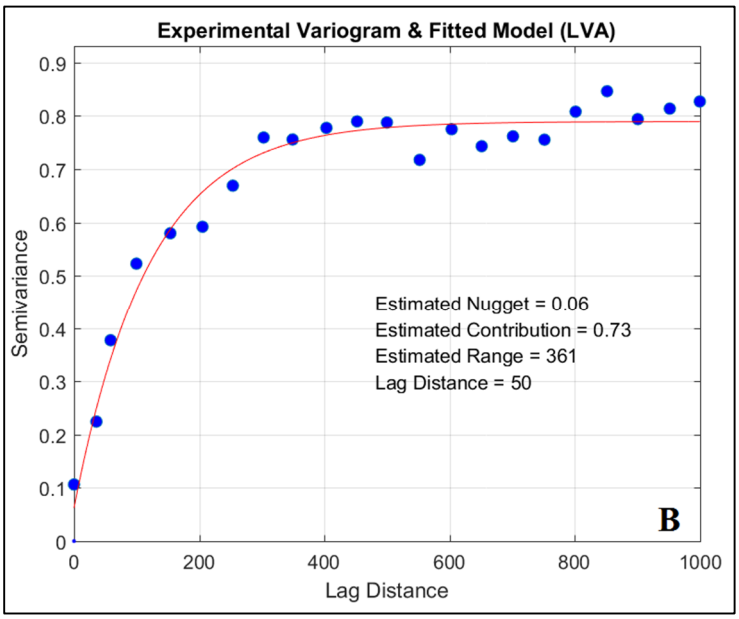

Figure 6. Parameters of the modeled variogram in presence of the LVA field.

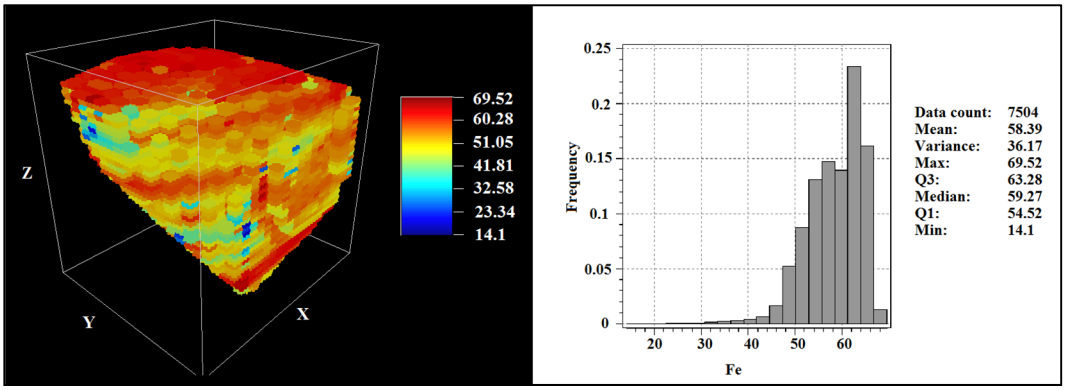

Figure 7. Left: Blocks of the studied area estimated with LVA-kriging. Right: histogram of the estimated data.

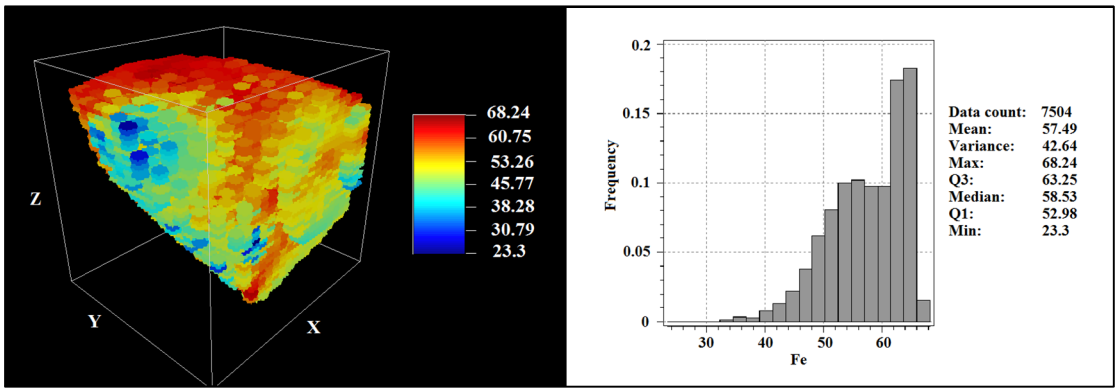

Figure 8. Modified blocks of the resources using ant colony algorithm.

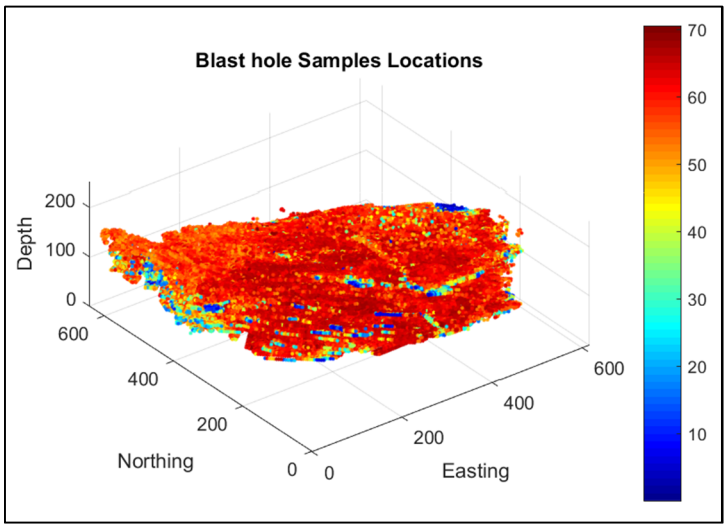

Figure 9. Blasthole samples in the studied area and their Fe (%) grade ranges.

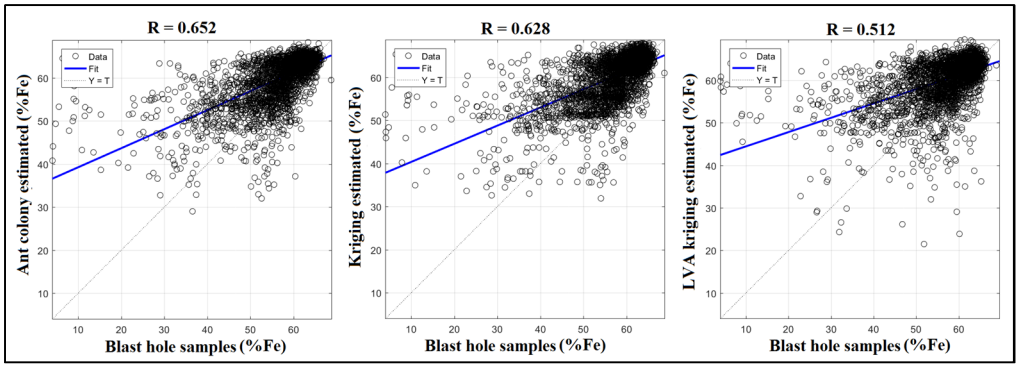

Figure 10. Validation plots of three estimation methods with blasthole samples.

The three methods were tested with the KL and JS divergences as well. The results obtained showed that again the ant colony system produced better outputs than the other two (Table 3).

Finally, the tonnage of the deposit was evaluated in equal cut-offs for three methods and presented using the mean grade cut-off grade (MG-CG) and tonnage cut-off grade (T-CG) curves (Figure 11). The curves are common tools in resource evaluation, which give information about the total contained tonnage or mean grade above a cut-off grade.

Table 3. KL and JS values used to evaluate the estimation methods.

	KL div.	JS div.
Conventional kriging	0.165	0.043
LVA-kriging	0.113	0.035
Ant Colony algorithm	0.057	0.025

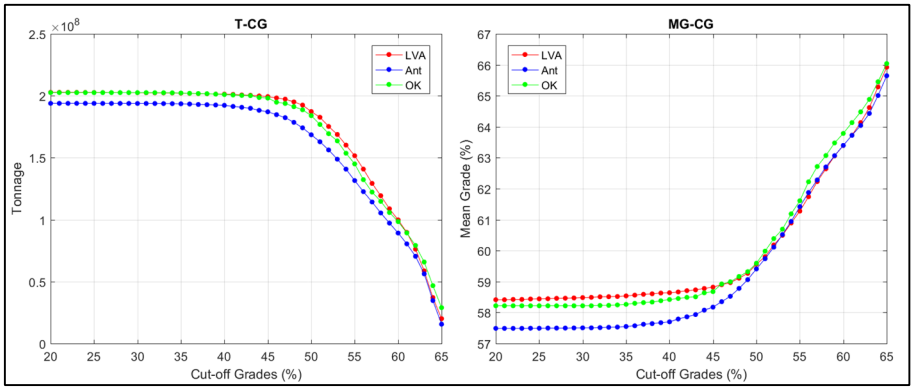

Figure 11. Estimated resource (left) and mean grades (right) with three methods in different cut-offs.

6. Discussion and conclusions

Conventional ordinary kriging is an inefficient estimator when the locally varying anisotropy exists. Many have tried to find non-linear solutions for estimating the deposits, especially with bedded, stratabound, stratiform, vein-type or layered forms. Boisvert [23] have presented LVA-kriging, which is the most recent attempt to consider local changes of continuity in the form of a field into kriging equations. Many researchers have also applied neural networks as the 'black box' on the data itself so that the final pattern of the reserve could be learned. Both approaches have some drawbacks. LVA-kriging requires an expert-based variography. Neural networks require sufficient data to learn the pattern, and their architecture has various parameters to be set.

One of the main goals of this work was to develop a new method for estimating resources in the presence of LVA with fewer complexities. The new approach uses the ACO algorithm to modify an interpolated image of the resource. The LVA field that is extracted from the available samples is used in the algorithm to direct the ants in more continuous grade paths. The paths are the cells/blocks that an ant passes in search for the higher grade values. The ants also act as moving average agents in their paths. The flexibilities of the ant colony compared to other swarm intelligence methods make it a favorable tool in optimizing the blocks.

The allowed maximum number of ants is equal to the number of cells in the grid. However, Zhuang suggested not to be less than square root of the number of cells as it would likely lead to an incomplete procedure [46]. Increasing the number of ants has no significant effect on the result but 1) a relative rise in the accumulated number of ants on the anisotropic routes and 2) more computer memory. An effective parameter is the number of iterations. It gives enough time to ants to complete their search process. The best choice is a high number of iterations. We tried with 5000, 10000, 20000, and 30000 but practically over 20000, the system stabled (Figure 12) and no active ants remained. The vertical axis indicates the number of ants that move in the grid. The more the algorithm proceeds, the fewer ants remain to move on to visit the blocks, and therefore, the less modification is done on the blocks.

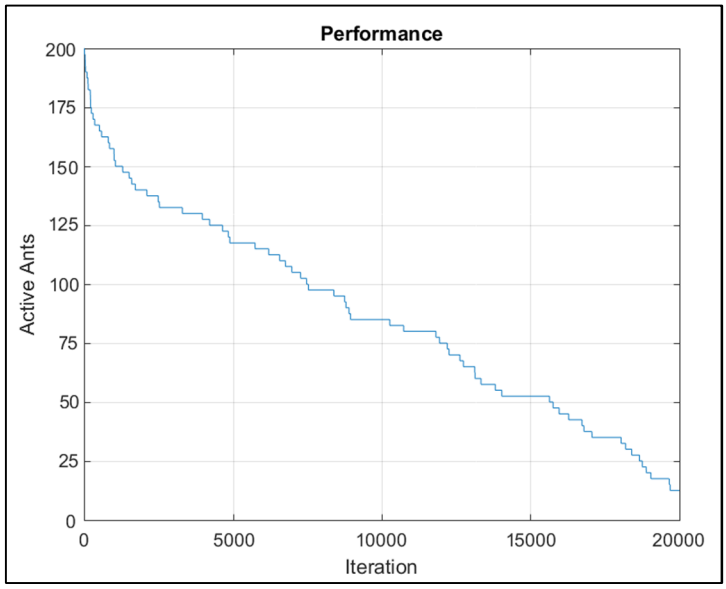

Figure 12. The active ants that move in the blocks in each iteration.

The initial values for pheromone trail and pheromone evaporation coefficient are chosen between 0 and 1, and have no significant influence on the result, although, as an experience, the values below 0.1 would make the ants find the minor anisotropic paths as well. Fluctuation limitation could be any number less than the lowest grid value.

Taboo path length is an important parameter as it would help an ant not to return to its current state repeatedly. The longer it is, the more grid points (or blocks) an ant can avoid to visit twice and the faster the iterative search process gets converged. We tried different lengths of Taboo: 10, 20, 30, 40, 50, 60, 70, and 80. The best result with the lowest JSD criterion was due to the length of 30.

Almost all the geostatistical estimation methods require a Gaussian normal distribution of samples, the condition that is not necessary for the ant colony estimation.

The tonnage-grade curves (Figure 11) reveal that the conventional and LVA kriging have overestimated the resource, especially in the lower cut-off grades, and show a higher tonnage and grade than the ant colony method. The reserve is estimated about 200 Mt at 20% Fe cut-off grade with the LVA and conventional kriging methods and about 190 Mt at the same cut-off with the ant-colony method (Figure 11, left). From the cut-off grade 50% upward (Figure 11, right), all the mean grade curves show almost a normal behavior and the three methods perform alike in high grades. That is due to the negative skewness of the grades and its tendency to higher grades.

In this case study, performance of the LVA kriging on the basis of validation was lower than the conventional kriging in comparison with the blast holes. However, LVA kriging could reproduce the initial distribution model (histogram) better than the conventional kriging on the basis of the JS divergence criterion. The LVA field production is a crucial step in LVA kriging, and if it was properly produced, e.g. on the basis of complementary data like geology and structural surveys, it could improve the results, especially in the structurally controlled deposits.

References

[1]. Deutsch, C.V. and Lewis, R. (1992). Advances in the practical implementation of indicator geostatistics. In: Proceedings of the 23rd International APCOM Symposium. pp 133-148.

[2]. Xu, W. (1996). Conditional curvilinear stochastic simulation using pixel-based algorithms. Math Geol. 28: 937-949.

[3]. Sullivan, J., Satchwell, S. and Ferrax, G. (2007). Grade estimation in the presence of trends-the adaptive search approach applied to the Andina Copper Deposit, Chile. In: Proceedings of the 33rd international symposium on the application of computers and operations research in the mineral industry. GECAMIN Ltd. pp 135-143.

[4]. Stroet, C. and Snepvangers, J. (2005). Mapping curvilinear structures with local anisotropy kriging. Math Geol. 37: 635-649.

[5]. Yao, T., Calvert, C. and Jones, T. (2007). Conditioning geologic models to local continuity azimuth in spectral simulation. Math Geol. 39: 349-354.

[6]. Almendral., A., Abrahamsen, P. and Hauge, R. (2008). Multidimensional scaling and anisotropic covariance functions. In: Proceedings of the Eighth International Geostatistics Congress. pp 187-196.

[7]. Sampson, P. and Guttorp, P. (1992). Nonparametric estimation of nonstationary spatial covariance structure. J Am Stat Assoc. 87: 108-119.

[8]. Brown, P., Le, N. and Zidek, J. (1994). Multivariate spatial interpolation and exposure to air pollutants. Can J Stat. 22: 489-509.

[9]. Meiring, W., Monestiez, P., Sampson, P.D. and Guttorp, P. (1997). Developments in the modeling of nonstationary spatial covariance structure from space-time monitoring data. Geostatistics Wollongong. 96: 162-173.

[10]. Perrin, O. and Meiring, W. (1999). Identifiability for non-stationary spatial structure. J Appl Probab. 36: 1244-1250.

[11]. Damian, D., Sampson, P.D. and Guttorp, P. (2001). Bayesian estimation of semi-parametric non-stationary spatial covariance structures. Environmetrics. 12: 161-178.

[12]. Schmidt, A.M. and O'Hagan, A. (2003). Bayesian inference for non-stationary spatial covariance structure via spatial deformations. J R Stat Soc Ser B (Statistical Method). 65: 743-758.

[13]. Higdon, D. (1998). A process-convolution approach to modelling temperatures in the North Atlantic Ocean. Environ Ecol Stat. 5: 173-190.

[14]. Higdon, D., Swall, J. and Kern, J. (1999). Non-stationary spatial modeling. Bayesian Stat. 6: 761-768.

[15]. Nott, D.J. and Dunsmuir, W. (2002). Estimation of nonstationary spatial covariance structure. Biometrika. 89: 819-829.

[16]. VerHoef, J.M., Peterson, E. and Theobald, D. (2006). Spatial statistical models that use flow and stream distance. Environ Ecol Stat. 13: 449-464.

[17]. Curriero, F.C. (2006). On the use of non-Euclidean distance measures in geostatistics. Math Geol. 38: 907-926.

[18]. Cressie, N. and Majure, J.J. (1997). Spatio-temporal statistical modeling of livestock waste in streams. J Agric Biol Environ Stat. pp. 24-47.

[19]. Little, L.S., Edwards, D. and Porter, D.E. (1997). Kriging in estuaries: as the crow flies, or as the fish swims? J Exp Mar Bio Ecol. 213: 1-11.

[20]. Rathbun, S.L. (1998). Spatial modeling in irregularly shaped regions: kriging estuaries. Environmetrics. 9: 109-129.

[21]. Løland, A. and Høst, G. (2003). Spatial covariance modeling in a complex coastal domain by multidimensional scaling. Environmetrics. 14: 307-321.

[22]. Krivoruchko, K. and Gribov, A. (2004).

Geostatistical interpolation and simulation in the presence of barriers. geoENV IV-Geostatistics Environ Appl. pp. 331-342.

[23]. Boisvert, J. (2010). Geostatistics with Locally Varying Anisotropy. PhD Thesis, University of Alberta.

[24]. Dorigo, M. (1992). Optimization, learning and natural algorithms. PhD Thesis, Politec di Milano.

[25]. Dorigo, M., Maniezzo, V. and Colorni, A. (1996). Ant system: optimization by a colony of cooperating agents. IEEE Trans Syst Man, Cybern Part B. 26: 29-41.

[26]. Stützle, T. and Hoos, H. (1998). Improvements on the ant-system: Introducing the MAX-MIN ant system. In: Artificial Neural Nets and Genetic Algorithms. pp. 245-249.

[27]. Liu, H., Abraham, A. and Clerc, M. (2007). An hybrid fuzzy variable neighborhood particle swarm optimization algorithm for solving quadratic assignment problems. J UCS. 13: 1309-1331.

[28]. Costa, D. and Hertz, A. (1997). Ants can colour graphs. J Oper Res Soc. 48: 295-305.

[29]. Bullnheimer, B., Hartl, R.F. and Strauss, C. (1999). An improved ant System algorithm for the vehicle Routing Problem. Ann Oper Res. 89: 319-328.

[30]. Gambardella, L.M., Taillard, É. and Agazzi, G. (1999). Macs-vrptw: A multiple colony system for vehicle routing problems with time windows. In: New ideas in optimization.

[31]. Ramos, V. and Almeida, F. (2004). Artificial ant colonies in digital image habitats-a mass behaviour effect study on pattern recognition. arXiv Prepr cs/0412086.

[32]. Wu, X. and Zhou, Y. (1993). Reserve estimation using neural network techniques. Comput Geosci. 19: 567-575.

[33]. Tahmasebi, P. and Hezarkhani, A. (2012). A hybrid neural networks-fuzzy logic-genetic algorithm for grade estimation. Comput Geosci. 42: 18-27.

[34]. Kapageridis, I. and Denby, B. (1998). Ore grade estimation with modular neural network systems-a case study. Inf Technol Miner Ind Ed by GN Panagiotou TN Michalakopoulos AA Balkema Publ Rotterdam. 52 P.

[35]. Chen, Y. and An, A. (2016). Application of ant colony algorithm to geochemical anomaly detection. J Geochemical Explor. 164: 75-85.

[36]. Sharifzadeh Lari, M., Fathianpour, N., Amir Fattahi, R. and Sadri, S. (2018). Improving Filtersim Simulation Algorithm of Multiple-Point Geostatistics Using New Training Image Based Adaptive Filters and Supervised Hard Data Conditioning. J Anal Numer Methods Min Eng. 8: 55-67.

[37]. Moore, F. and Modabberi, S. (2003). Origin of Choghart iron oxide deposit, Bafq mining district, Central Iran: new isotopic and geochemical evidence. J Sci Islam Repub Iran. 14: 259-270.

[38]. Foerster, H. and Jafarzadeh, A. (1994). The Bafq mining district in central Iran; a highly mineralized Infracambrian volcanic field. Econ Geol. 89: 1697-1721.

[39]. Torab, F.M. and Lehmann, B. (2006). Iron oxide-apatite deposits of the Bafq district, Central Iran: an overview from geology to mining. World Min- Surf & Underground. 58: 355.

[40]. Mohammadhassanpour, R. (2007). Tools for multivariate modeling of permeability tensors and geometric parameters for unstructured grids. In: Masters Abstracts International.

[41]. Lillah, M. and Boisvert, J.B. (2015). Inference of locally varying anisotropy fields from diverse data sources. Comput Geosci. 82: 170-182.

[42]. Boisvert, J.B. and Deutsch, C.V. (2011). Programs for kriging and sequential Gaussian simulation with locally varying anisotropy using non-Euclidean distances. Comput Geosci. 37: 495-510.

[43]. Yang, X.S. (2010). Nature-inspired metaheuristic algorithms. Luniver press.

[44]. Kullback, S. and Leibler, R.A. (1951). On information and sufficiency. Ann Math Stat. 22: 79-86.

[45]. Honarkhah, M. and Caers, J. (2010). Stochastic simulation of patterns using distance-based pattern modeling. Math Geosci. 42: 487-517.

[46]. Zhuang, X. (2004). Image feature extraction with the perceptual graph based on the ant colony system. In 2004 IEEE International Conference on Systems, Man and Cybernetics (IEEE Cat. No. 04CH37583) (Vol. 7, pp. 6354-6359). IEEE.

الگوریتم کولونی مورچگان به عنوان یک روش با راندمان بالا در تخمین ذخیره به کمک میدان LVA؛ مطالعه موردی: کانسار سنگ‌آهن چغارت

حمید معینی و فرهاد محمدتراب*

دانشکده مهندسی معدن و متالورژی، دانشگاه یزد، ایران

ارسال ۲۰۱۸/۱۲/۲۹، پذیرش ۲۰۱۹/۴/۱۲

* نویسنده مسئول مکاتبات: fmtorab@yazd.ac.ir

چکیده:

کریجینگ یک روش زمین‌آماری پیشرفته است که یک سطح یا مدل سه‌بعدی تخمینی را از روی مجموعه‌ای از نقاط پراکنده تولید می‌کند. این روش می‌تواند در تخمین ذخایر معدنی با استفاده از یک شبکه حفاری نمونه‌برداری شده به کار رود. با این وجود، روش مرسوم کریجینگ (OK) قادر به تأثیردهی ناهمسانگردی موضعی متغیر (LVA) نیست. در روش ارائه شده، یک میدان LVA با محاسبه پارامترهای ناهمسانگردی در هر سلول شبکه تخمین، ساخته می‌شود. پس از تبدیل کوتاه‌ترین فاصله‌های ناهمسانگردی بین نمونه‌ها (با کمک میدان LVA به دست آمده) به فاصله‌های اقلیدسی، از ماتریس فاصله مذکور در واریوگرافی و کریجینگ (LVAOK) استفاده می‌شود. الگوریتم بهینه‌سازی کولونی مورچگان (ACO) یک روش فرا ابتکاری برگرفته از طبیعت است که تاکنون در زمینه‌های مختلف از جمله استخراج ویژگی‌های تصویر و تشخیص آنومالی ژئوشیمیایی استفاده شده است. برنامه‌ای بر اساس ACO طراحی شد تا مورچه‌ها با قرارگیری در شبکه تصویر اولیه از عیارها، مسیرشان را منطبق بر پارامترهای میدان LVA انتخاب و در نهایت هرکدام به صورت یک عامل میانگین متحرک عمل کنند. اگر پارامترهای آغازین الگوریتم ACO به درستی انتخاب شوند، مورچه‌ها قادر خواهند بود مسیرهای کانی‌سازی را شبیه‌سازی کرده و تصویر نهایی اصلاح شده مطابق با ناهمسانگردی عیاری اصلاح شود. در این پژوهش، کانسار آهن چغارت با ۲۴۴۷ نمونه کامپوزیت گمانه‌های اکتشافی به روش‌های LVAOK و ACO مطالعه شد. نتایج با ۱۱۱۱۳۱ نمونه چال آتشباری و نیز معیار جنسون- شانون (JS) اعتبارسنجی شد و نشان داد که ACO از هر دو روش LVAOK و OK بهتر عمل کرده است (با ضریب همبستگی ۰/۶۵ و JS ۰/۰۲۵). تنها نقطه ضعف ACO پارامترهای آن است که به صورت سعی و خطا انتخاب می‌شوند.

کلمات کلیدی: الگوریتم کولونی مورچگان، ناهمسانگردی موضعی متغیر، تخمین ذخیره، کریجینگ، کانسار چغارت.